Adenovirus 5 Recovery Using Nanofiber Ion Exchange Adsorbents

Jordan Turnbull,[1] Bernice Wright,[1] Nicola K Green,[2] Richard Tarrant,[2] Iwan Roberts,[3] Oliver Hardick,[3] Daniel G. Bracewell[1]

[1]Department of Biochemical Engineering, University College London, Bernard Katz Building, Gower Street, London WC1E 6BT, United Kingdom; telephone: +44 20 7679 9580; d.bracewell@ucl.ac.uk

[2]Clinical BioManufacturing Facility, University of Oxford, Old Road, Headington, Oxford, OX3 7JT, United Kingdom

[3]Puridify, Stevenage Bioscience Catalyst, SG1 2FX, United Kingdom

Grant Numbers

EP/L01520X/1 and EP/N013395/1

Abstract

Viral vectors such as adenovirus have successful applications in vaccines and gene therapy but the manufacture of high quality virus remains a challenge. It is desirable to use the adsorption based chromatographic separations that so effectively underpin therapeutic protein manufacture. However fundamental differences in the size and stability of this class of product means it is necessary to revisit the design of sorbent's morphology and surface chemistry. In this study, the behaviour of a cellulose nanofiber ion exchange sorbent derivatised with quaternary (Q) amine ligands at defined densities is characterised to address this. This material was selected as it has a large accessible surface area for viral particles and rapid process times.

Initially the impact of surface chemistry on infective product recovery using low (440 µmol/g), medium (750 µmol/g) and high (1029 µmol/g) ligand densities is studied. At higher densities product stability is reduced, this effect increased with prolonged adsorption durations of 24 minutes with just ~10% loss at low ligand density vs. ~50% at high. This could be mitigated by using a high flowrate to reduce the cycle time to ~1 minute. Next the impact of ligand density on the separation's resolution was evaluated. Key to understanding virus quality is the virus particle: infectious virus particle ratio. It was found this parameter could be manipulated using ligand density and elution strategy. Together this provides a basis for viral vector separations that allows for their typically low titres and labile nature by using high liquid velocity to minimise both load and on-column times while separating key product and process related impurities.

Keywords

Nanofibers, anion exchange chromatography, viral vectors, downstream processing

Introduction

The adenovirus serotype 5 (Ad5) particle is a non-enveloped, icosahedral capsid with a 90-100 nm diameter that carries a linear, double-stranded DNA genome (San Martin, 2012). Human Ad5 is the most widely studied adenovirus serotype and is a typical model for viral vector process development (Crystal, 2014). Ad5 is an attractive gene delivery vector due to structural stability, ability to carry large transgene payloads and broad tissue tropism (Crystal, 2014). As of 2017, 20% of all gene therapy trials utilise an adenovirus vector (Lee et al., 2017). In the majority of these clinical trials the Ad5 vector fulfils two roles; in an oncolytic capacity for treatment of cancers and as a vaccine whereby the vector expresses a foreign antigenic protein (Keeler, ElMallah, & Flotte, 2017).

Downstream processing of viral vectors represents a significant bottleneck and a primary cost of production (Vellinga et al., 2014). Conventionally, industry and academia have relied heavily on the ultracentrifugation technique for downstream purification of highly purified viral vectors (Chen, Marino, & Ho, 2016). However, the process has major drawbacks including poor scalability and high operating costs (Vicente, Roldão, Peixoto, Carrondo, & Alves, 2011).

Initial efforts to develop scalable purification platforms led to the repurposing of anion-exchange resins designed for protein purification, building on experience of therapeutic protein processes. Increases in the physical size and complexity of biological products such

as viral vectors highlight the limitations of these conventional resin-based chromatographic platforms, for instance poor recovery of the complex biotherapeutics (Lucero et al., 2017).

To address this, a number of alternative chromatography materials have been applied to the purification of viruses designed to improve the efficiency and scalability of the process. Monoliths have been applied to Ad5 purification (Whitfield, Battom, Barut, Gilham, & Ball, 2009) as well as the separation of much larger enveloped virus species including Vaccinia viruses (350 nm) (Vincent et al., 2017). The recovery of a recombinant Ad5 gene therapy was improved from 28% using a Q-Sepharose™ XL column to 35% using a monolith column (CIM™ QA-1) (Lucero et al., 2017). Previous reports showed that the CIM™ QA-1 was preferable over the weak anion CIM™ DEAE-1. The final infective coefficient of virus particle per infective virus particles (VP/IVP) was 13, a range documented as acceptable for potency by the Food and Drug Administration (Kramberger, Urbas, & Štrancar, 2015). Other work using a porous cast membrane Peixoto, Ferreira, Sousa, Carrondo, and Alves (2008) achieved a 62% recovery (determined by cell fluorescence) of infectious Ad5. As well as exploration of alternate adsorbents there has also been a significant amount of work to optimise process and platform design. Piergiuseppe Nestola et al. (2014) described purification of Ad5 using a two column, quasi-continuous, simulated moving-bed size exclusion chromatography (SEC) process which achieved a recovery of 86% determined by real-time PCR.

In the this work nanofibers adsorbents are used which have seen a variety of separation applications and can be synthesised in a range of materials such as nylon (Stanelle, M Straut, & Marcus, 2007), glass and cellulose (Ruckenstein & Guo, 2004). The cellulose

nanofiber based adsorbents used exhibit a number of physical properties which could be beneficial for Ad5 purification when compared to existing commercial monolith/resin/membranes, including their high surface area and mobile phase accessibility to the entire functionalised surface. Ryu, Kim, Lee, Park, and Lee (2003) reported surface areas of 14 m^2g^{-1} for nylon 6 nanofibers and poly(4-vinylpyridine) nanofibers were shown to have an area of 26 m^2g^{-1} (Matsumoto, Wakamatsu, Minagawa, & Tanioka, 2006). Porous cast membranes for bioseparations with a pore size of 0.45 µm exhibit a surface area of 1-2 m^2g^{-1} a surface significantly lower than nanofibers (Wang, Faber, & Ulbricht, 2009). Beaded porous resins typically have the highest reported surface area at 40 m^2g^{-1} (Wen-Chien, Chang-Hung, Ruoh-Chyu, & Keh-Ying, 1995). Despite the high surface area of these resins, the pore size (typically less than 100 nm) results in size exclusion of Ad5 from the inner functionalised surface resulting in lower binding capacities (Lusky, 2005) for large biological product such as viruses than would otherwise be expected. The electrospinning process that is used to fabricate the nanofibers requires controlled atmospheric conditions in order to generate consistent nanofiber deposition. Using this approach an average nanofiber diameter within 5% of 350 nm (Hardick, Stevens, & Bracewell, 2011) can be achieved. The fibres are randomly deposited (non-woven) to create a consistent stationary phase architecture to avoid channelling while keeping favourable pressure and flow characteristics (Hardick et al., 2011). The resulting adsorbent bed once derivatised with an appropriate ligand and packed has convective mass transfer characteristics, and an internal porosity estimated to be 0.62 by mass-density-volume calculations. In this work the nanofibers are packed in a ~0.125 mL bed (height 0.3 mm, diameter 25 mm) (Hardick, Dods, Stevens, & Bracewell, 2013).

To create nanofibers with the desired separation properties for this use ligand density on the adsorbents is critical. Vicente, Fáber, Alves, Carrondo, and Mota (2011) demonstrated this parameter impacted recombinant baculovirus (rBV) product quality and impurity clearance for anion exchange membranes. P. Nestola et al. (2014) have shown on similar adsorbents that Ad5 recovery is doubled by reducing the grafted ligand density. In the current study, nanofibers incorporating Q amine ligands at low, medium and high densities on the adsorbent surfaces are used. It is hypothesised that modifying the density of the ligand in this manner would affect Ad5 binding and separation of product and process related impurities, as well as yield.

Materials and Methods

Materials

The HEK293 cell line used for the generation of Ad5 stocks and for performing the β-galactosidase infectivity titre were purchased from American Tissue Culture Collection (Manassas, VA, USA). Ad5containing a β-galactosidase gene insert were kindly gifted from the Clinical BioManufacturing Facility (Oxford, UK). Nanofiber adsorbents were made to a range of Q amine ligand densities of low (440 µmol/g), medium (750 µmol/g) and high (1029 µmol/g) quaternary (Q) ligand density nanofibers by Puridify (now GE Healthcare, Stevenage, UK). All chemicals were purchased from Sigma-Aldrich (Poole, UK) unless otherwise stated. Antibodies for Western blotting analyses were purchased from Abcam or 2BScientific. Polyclonal antibody - Primary antibody: Rabbit polyclonal antibody to Ad5 (catalogue number: ab6982, Abcam, Cambridge, UK), secondary antibody: Goat polyclonal antibody to rabbit IgG (catalogue number: ab6721, Abcam, Cambridge, UK). Ad5 Hexon

antibody - Mouse monoclonal antibody to Ad5 Hexon (catalogue number: 10R-8460 2BScientific Limited, Upper Heyford, UK), secondary antibody: Rabbit polyclonal antibody to mouse IgG (catalogue number: ab6728, Abcam, Cambridge, UK).

Methods

HEK293 Cell Culture

HEK293 cells were cultured in an incubator at 37°C in a 5% (v/v) CO_2 enriched atmosphere at 95% humidity. Cells were cultured for three days and passaged at 80% confluency. Cells were counted using a haemocytometer and they were cultured in Dulbecco's Modified Eagle's Medium from Life Technologies (catalogue no: 21969035, Paisley, UK) supplemented with 10% (v/v) foetal bovine serum (Sigma-Aldrich, Steinheim, Germany), 1% (v/v) penicillin/streptomycin (Life Technologies, Paisley, UK), and 2 mM L-glutamine (Biochrom, Cambridge, UK). Cells were cultured in 10-tiered HYPERFlasks® (Sigma-Aldrich, Steinheim, Germany).

Adenovirus 5 Propagation in HEK293 Cells

Infection of HEK293 cells with Ad5 was performed by adding 100 μL, 5.1 x 10^9 VP of Ad5 in 2.5% glycerol to HYPERFlasks® containing HEK293 cells at 80% confluency. The cells were then incubated for 48 h in the cell culture incubator at 37°C, 5% (v/v) CO_2 and 95% humidity.

Adenovirus 5 Harvest and Clarification

To harvest Ad5 propagated in HEK293 cells, the HYPERFlasks® were knocked, removing the cells from culture surface, and the contents transferred to 50 mL centrifuge tubes. Cells

were stored on dry ice for 30 min and thawed at 37°C for 40 min. The cycle of freezing and thawing was performed three times to disrupt the cell membrane (Lucero et al., 2017). The cell lysate was then centrifuged at 2,000 rpm for 10 min, and filtered using 33 mm Polyethersulfone (PES) membrane sterile syringe driven filters (0.45µm, Merck Millipore, Feltham, UK) and pooled. Tangential flow filtration (TFF) of the clarified cell lysate (CCL) was conducted on a KR2*i* system using a 500 kDa molecular weight cut off (MWCO) D06-E500-05-N hollow fiber (length 65 cm, surface area 370 cm^2; both Spectrum Labs, Breda, The Netherlands) at a flow rate of 20 mL/min and transmembrane pressure of 2 Psi (± 0.5). The cell lysate was concentrated 4X and dialysed in binding buffer (20 mM Tris, pH 7.4) 5X volume of retentate, sample was then diluted 1 in 4 to original harvest volume to control for changes in loading volume when comparing TFF and CCL feed.

Scanning Electron Microscopy Analysis of Adenovirus 5 Binding to Quaternary Amine Functionalised Nanofibers

Quaternary amine functionalised nanofiber disks were washed with ddH_2O and submerged in an aqueous binding buffer containing 20 mM Tris pH 7.4. The nanofibers were then conditioned in fresh binding buffer for 30 min. Clarified Ad5 (~10^9 VP: 100 µL) in culture media was added to 900 µL fresh binding buffer to which the discs were submerged and agitated at room temperature for 60 min. A selection from this sample of nanofiber disks were washed in binding buffer to remove non-bound material and submerged in 1% (v/v) glutaraldehyde solution for 10 seconds and left to dry at room temperature. A second batch of nanofiber disks were prepared as before and then submerged in 20 mM Tris, 1 M NaCl pH 7.4 for 5 minutes, the nanofibers were then washed with ddH2O and submerged in 1%

(v/v) glutaraldehyde aqueous solution for 10 s and dried at room temperature. Scanning electron microscopy (SEM) was used to image the virus particles bound the adsorbent, the open structure of nanofibers meant that no manipulation of the nanofiber bed was required to visualise adsorbent surface. Nanofibers were mounted on aluminium stubs using adhesive carbon taps. Mounted samples were coated in a 2 nm layer of gold/palladium using a 681 Gatan ion beam coater (Roper Industries, Abingdon UK) and imaged using a JEOL 7401 FEGSEM (JEOL, Peabody, MA US).

Chromatography

Two different Ad5 containing feeds were assessed to determine if a reduction in process impurities achieved by incorporating a TFF step into the process would change the feed binding characteristics on nanofiber membranes. Two feeds were prepared. One a cell lysate clarified by 33 mm Polyethersulfone (PES) membrane sterile syringe driven filters (0.45µm, Merck Millipore, Feltham, UK), referred to as clarified cell lysate (CCL). The second feed was prepared taking CCL then processed using TFF, referred to as 'TFF'. Experiments were performed using an ÄKTA Avant (GE Healthcare Life Sciences, Buckinghamshire UK), with online measurements of pH, conductivity and UV absorbance (260 and 280 nm). The ~0.125 mL nanofiber adsorbent (bed height 0.3 mm, diameter 25 mm) was equilibrated with 10 mL wash buffer containing 20 mM Tris, pH 7.4 at a flow rate of 10 mL/min. 5 mL Ad5 feed at a concentration of ~10^8 filled virions per mL (VP/mL) was loaded onto the nanofiber adsorbent that was washed with binding buffer until conductivity reached a constant reading. A linear 20 mL gradient elution (20 mM Tris, 1 M NaCl, pH 7.4) was applied to

nanofibers at a flow rate of 10 mL/min to elute Ad5 bound to the nanofiber adsorbent. The nanofiber adsorbent was washed with 2 M NaCl 20 mM Tris, pH 7.4.

To investigate the effect of prolonged adsorption durations on Ad5, 5 mL of CCL was loaded onto the nanofiber and wash steps were performed with 10, 40, 80 or 240 mL equilibration buffer at a flow rate of 10 mL/min. Peak resolution was determined by identifying peaks from 20 mL gradient elutions and a step elution methodology was developed using the relative salt concentrations identified.

The resolution of peaks was refined by extending the gradient elutions when multiple peaks with similar isoelectric points were identified. Total run time for step elution was limited, whilst maintaining a constant flow rate of 10 mL/min, to minimise any potential effects of prolonged adsorption durations on Ad5 infective recovery whilst allowing high resolution separations. Elution fractions were collected using a F9-R fraction collector (GE Healthcare Life Sciences, Buckinghamshire UK). All samples were diluted 1 in 7.5 in phosphate buffered saline to minimise the effects of high salt on recovery of infective Ad5 particles.

Western Blotting

Fractions were concentrated using Vivaspin® Turbo 4 (Sartorius, Gottingen Germany). Total protein was quantified using the Modified Lowry protein assay according to manufacturer's instructions (ThermoFischer, East Grinstead, UK). Protein samples were treated 1:1 with Laemmli sample treatment buffer: 50 mM Tris-HCl, 4% (w/v) SDS (Sigma), 10% (v/v) β-mercaptoethanol (Sigma), 20% (v/v) glycerol (Sigma), a trace of Coomassie brilliant blue R (Sigma), pH 6.8, and heated at 95°C for 5 min. Proteins were

separated via SDS-PAGE using NuPAGE™ precast 10%, BisTris mini-gels (ThermoFischer, East Grinstead, UK) with gels run at 100 V per gel. Proteins were transferred from gels to polyvinylidine difluoride membranes using an iBlot™ 2 gel transfer device following the manufacturer's instructions. Blots were blocked with 5% milk (w/v) for 1 h at room temperature before they were incubated in primary antibody (mouse monoclonal antibody to Ad5 hexon in 2% milk (w/v)) overnight at +4°C. Blots were washed three times in 1X tris buffered saline-tween (TBS-T) for 5 min before incubating in secondary antibody (rabbit polyclonal antibody to mouse IgG (HRP-conjugated) in 2% milk) for 2 h at room temperature. Blots were imaged after a 1 min incubation in enhanced chemiluminescent reagent using an Amersham Imager 600 (GE Healthcare Life Sciences, Buckinghamshire UK).

Analysis of Purified Adenovirus 5 using Transmission Electron Microscopy

Transmission electron microscopy was used to visualise Ad5. To perform the analysis, Ad5 particles were negatively stained by adding uranyl acetate to Ad5 samples. The stained samples were dropped onto a carbon grid (400 mesh) and loaded onto JEOL 1010 Transmission Electron Microscope (JEOL, Peabody, MA USA) before they were imaged.

Host Cell Protein Quantification

Host cell protein (HCP) concentrations from purified Ad5 fractions were analysed using the HEK293 HCP ELISA kit F650R (Cygnus Technologies, Southport, NC, USA) following manufacturer's instructions.

Quantitative PCR

To assess total Ad5 capsids containing DNA, samples were analysed using Adeno-X™ Rapid Titer Kit (Takara Bio Europe, Saint-Germain-en-Laye, France). Briefly, samples were pre-treated with DNAase to remove ex-virus DNA, and then chemically lysed with protease; DNA was isolated using NucleoSpin® Virus Columns (Takara Bio Europe, Saint-Germain-en-Laye, France). Samples were added to master reaction mix in a 96 well plate so that each well contained 2 µL of unknown sample or standard control DNA, 6.8 µL PCR-grade H_2O, 0.4 µL Adeno-X forward primer (10 µM), 0.4 µL Adeno-X reverse primer (10 µM), 0.4 µL ROX™ Reference Dye LMP, 10.0 µL SYBR® Advantage qPCR Premix. All reaction were performed using a CFX Connect™ Real-Time PCR Detection System (Applied Biosystems, CA, USA) using the following cycle conditions: stage one, 95°C for 30 seconds; stage two, 95°C for 5 seconds, followed by 60°C for 30 seconds (40 repetitions); stage three, dissociation curve of 95°C for 10 seconds, 65°C to 95°C increment 0.5°C every 5 seconds. To ensure that recoveries obtained from NucleoSpin® Virus Columns (Takara Bio Europe, Saint-Germain-en-Laye, France) were not affected by the range of salt conditions present in the elution samples, a range of samples containing standard control DNA containing 20 mM Tris, and a range of salt concentrations from 0-0.5 M NaCl (all pH 7.4) were also analysed.

Adenovirus 5 Cell Infectivity Assay

The detection and quantification of Ad5 units that were able to deliver the β-galactosidase gene were analysed as a measure of sample infectivity using the β-galactosidase reporter gene staining kit (Sigma-Aldrich, Taufkirchen Germany). Reactions were conducted

following manufacturer's instructions but they were modified for a 96-well plate format. Briefly, plates were coated in poly-L-lysine for 10 min. HEK293 cell suspension of concentration of 4 x 10^5 cells per mL were loaded per well and incubated overnight. Growth media was removed from wells prior to transfection with serial dilutions of Ad5 (100 µL of Ad5 sample in supplemented DMEM) and the plate incubated for 1 h at 37°C. The Ad5 sample was then removed from wells, replaced with 100 µL of growth media and the plate was incubated overnight at 37°C. To stain, media was removed from wells and cells (attached to well surfaces) were washed twice with phosphate buffered saline (PBS), fixed with 1X fixation buffer (20% formaldehyde, 2% glutaraldehyde in 10X PBS) and incubated for 10 min at room temperature. Wells were washed twice with PBS followed by 30 µL of staining solution. Plates were incubated at 37°C for 24 h and blue stained cells were manually counted using a light microscope.

Results and Discussion

Binding and Elution of Adenovirus 5 under Batch Conditions

Batch experiments were conducted to gain insight into the mechanism for virus binding with the purification materials (Wickramasinghe, Carlson, Teske, Hubbuch, & Ulbricht, 2006). Direct imaging of bound virus particles was conducted using scanning electron microscopy (SEM) to determine if the binding and elution interaction behaved as expected using previously described buffer conditions (Peixoto et al., 2008). Adenovirus 5 particles were bound to anion exchange nanofibers under batch conditions by submerging nanofiber disks into binding buffer containing the virus. The nanofibers were then imaged using SEM (Figure 1). Adenovirus 5 virions measure ~90 nm in diameter and are clearly visible bound

to the nanofiber adsorbent. Other host cell components are also visible as a layer bound to the nanofiber surface. To determine if product and impurity components had migrated into the inner bed structure as expected several cross sections through the nanofiber bed were imaged with no observable differences between layers (data not shown). To elute the bound virus, nanofibers were submerged in high salt (1 M NaCl, 20 mM Tris, pH 7.4) elution buffer subsequent SEM reveals all components were visibly removed from the nanofiber surface (Figure 1).

Comparison of Clarified and Buffer Dialysed Adenovirus 5 Feeds

Adenovirus 5 harvest was clarified with 0.45 µm filters, this clarified cell lysate (CCL) was divided - 50% was further processed using ultrafiltration and diafiltration (UF–DF) with a 500 kDa TFF system to retain Ad5 and remove bulk host cell impurities before dialysis into binding buffer. The TFF and CCL feeds were analysed using the β-galactosidase infectivity assay to characterise the effect of processing on Ad5 infective potency. After TFF filtration the retentate had an infective recovery of 89% compared to the CCL.

A 5 mL ($5.6 \times 10^8 \pm 5.6 \times 10^7$ IVP) volume of CCL Ad5 feed was loaded onto a 0.125 mL anion exchange nanofiber adsorbent at 10 mL/min (Figure 2), and a 20 mL gradient elution of up to 1 M NaCl was applied to the column. The elution profile was then compared to a 5 mL ($5.6 \times 10^8 \pm 5.6 \times 10^7$ IVP) load of TFF feed under the same process conditions. This was repeated for low, medium and high density Q amine ligand nanofibers. A large flow through peak was observed for all the ligand densities when challenged with CCL feed. This was not observed for the TFF feed, due to the removal of impurities during the TFF step. The total UV peak area for the TFF feed is reduced compared to the CCL feed, again due to

clearance of host cell impurities. Comparison of the CCL feed across the three different Q amine nanofibers (low, medium and high ligand density) shows elution profiles are distinct across all three fiber types (Figure 2), with components binding more tightly giving rise to more peaks and requiring higher ionic strength to elute as ligand density increases. There are more subtle differences seen for the TFF treated material, which are more noticeable at the highest charge density. An explanation could be that with the reduced impurity levels present in the TFF material interactions between Ad5, impurities and the charge surface that allow discrimination for the CCL material are reduced. The distinct elution profile across the three fiber types, demonstrate different separation capabilities of nanofibers as the Q amine ligand density changes. This suggests that by tailoring the ligand functionalisation of the nanofibers it is possible to optimise Ad5 purification process for improved separations.

Extended Adsorption Periods on Quaternary Amine Functionalised Nanofibers Reduce Adenovirus 5 Infectivity

Poor viral vector recoveries over an ion exchange chromatography step have been attributed to prolonged adsorption periods that cause degradation of capsid integrity and entrapment of virus particles in the complex internal adsorbent structures (Trilisky & Lenhoff, 2009). Hardick et al. (2013) showed that the large inter-fiber space and morphology of the functionalised surface of nanofibers minimises diffusive mass transfer limitations, a property which has been shown to be detrimental to capacity and recovery of large biotherapeutic molecules (Wickramasinghe et al., 2006). This open structure (Figure 1) may minimise entrapment events and multipoint attachment, suggesting loss in infective units is a result of irreversible binding or capsid damage.

The effects of prolonged binding duration on the recovery of infective Ad5 (Figure 3) was analysed. CCL clarified Ad5 feed (5 mL) was loaded onto nanofiber columns and adsorption durations were selected to approximately replicate binding durations of current chromatographic viral vector manufacturing processes. Figure 4 shows overlay chromatograms for low ligand density 1, 4, 8 and 24 min adsorption periods. A 100% recovery of infective virus was observed after the shortest binding duration (1 min) using low ligand density nanofibers (Figure 3). Extending binding durations from 4-24 min using low ligand density nanofibers did not cause a significant decrease in the infectivity of Ad5 eluate, with recoveries between 87-90%. At an extended adsorption duration of 24 min there was a dramatic loss of almost 50% in total infective capsids for medium and high ligand density nanofibers. Significant losses in Ad5 infective recoveries were also observed on high ligand density nanofibers after adsorption periods of 1-8 min and 8-24 min adsorption periods.

The substantial losses in Ad5 infectivity observed with use of the medium and high ligand density nanofibers indicates product damage. This could be a result of loss of critical features of the virus for its infectivity, i.e. fiber proteins (McNally, Darling, Farzaneh, Levison, & Slater, 2014). Alternatively the loss of infective units could be caused due to deformation of the capsid as it is 'pulled' onto the functionalised surface over the adsorption duration, damaging the capsid. Similar effects have been observed during the recovery of virus-like particles of recombinant hepatitis B virus surface antigen (Huang et al., 2006). This is of particular relevance for Ad5 as Perez-Berna et al. (2012) have shown that the virus maturation process gives rise to a metastable structure. These brittle capsids may show

a reduced resistance to multipoint attachment, when compared to immature non-infective Ad5. These data suggest that although medium and high ligand density nanofibers limit the recovery of infective Ad5 over extended adsorption periods, acceptable recovery can be achieved if the rapid bind/elute times possible with these nanofiber adsorbents is utilised.

Quaternary Amine Functionalised Nanofibers Achieve Efficient, High Yield Purification of Infectious Adenovirus 5 Particles

Vicente, Fáber, et al. (2011) reported that ligand density caused a larger change in binding capacity for a protein (bovine serum albumin) when compared to either a phage (rBV) or virus (Ad5). To investigate whether an impact could be seen on Q functionalised nanofibers three ligand densities were exposed to a greater vector load challenge. Here the nanofiber column volume (CV) 0.125 mL, was loaded with 50 mL (400 CV) TFF processed Ad5 feed (total load 2.39 x 10^{10} VP, 5.6 x 10^{9} IVP) (Figure 5). Five 10 mL flowthrough fractions were collected from each run and screened for the presence of infective Ad5 capsids. No infective Ad5 capsids were present in the flowthrough (data not shown) which indicates that capacity was not reached. Therefore we performed a Fermi estimate to understand what the limit of capacity for viral particles this nanofiber adsorbent system is likely to be capable of. Based on the SEM image (Figure 1) it was conservatively assumed 25 viral particles are bound per micron of nanofiber and calculating in the region of 5,000 km of nanofiber to be present in a 1 mL packed bed we determined a capacity 1.25 x 10^{14} VP/mL. The load challenge of 1.78 x 10^{11} VP/mL used in this study is far lower than this calculated capacity and exceeds what we were able to test in this study. Indeed in such a low titre vector manufacturing process the dynamic binding capacity (DBC) would likely not be reached as many 1,000s of CVs

would be required, even when considering the contribution of impurity binding in a well-designed ion exchange step.

In vivo therapeutic loads of Ad5 range from 10^8 to 10^{12} virus particles (VP) per dose depending on the therapy and site of administration (Habib et al., 2001; Smaill et al., 2013). Whilst further work to determine the upper limit of capacity is required at the current scale, a single 0.125 mL column can recover ten 10^9 VP doses per cycle. Operating at 10 mL/min (4,800 CV/h), a conservative flowrate for this adsorbent with an 80 mL full cycle, the nanofibers exhibit a productivity of 1.43 x 10^{15} VP/L/h. In comparison a 1 mL Sepharose Q XL column operating at 0.5 mL/min was shown to have an Ad5 DBC of 1.30 x 10^{11} VP by Bo et al. (2015) which gives rise to a productivity of 4.88 x 10^{13} VP/L/h. Under these assumptions nanofibers exhibit a 29-fold increase in productivity compared to conventional packed bed resins.

This compares favourably with Hardick, Dods, Stevens, and Bracewell (2015) where it is shown nanofibers are capable of operating at high flow rates to increase protein purification productivity, achieving a 15-fold increase compared to packed bed adsorbents. Running the Ad5 separation at this higher velocity (70 mL/min) shows no significant impact on Ad5 infective recovery (data not shown). Operating under these conditions nanofibers could achieve a productivity of 1 x 10^{16} VP/L/h.

Reproducibility and Life Cycle Performance of Quaternary Amine Functionalised Nanofibers

High performance and reproducible performance of chromatography tools are paramount in bioprocessing (Rathore & Sofer, 2005). Nine consecutive bind/elute profiles for each nanofiber ligand density were compared to demonstrate operational reproducibility. There was no detectable loss in binding capacity after nine runs across all three nanofiber ligand densities suggesting a 2 M NaCl wash was sufficient to remove TFF Ad5 feed components between runs (data not shown). The absorbance flow profiles were then compared to two more nanofiber cartridges of the same chemistry to demonstrate manufacturing reproducibility. Peak area variability of <5% was observed between cartridges suggesting good manufacturing reproducibility (data not shown).

Separation of Infectious Adenovirus 5 Particles Using Quaternary Amine Functionalised Nanofibers

High infective product recovery is the primary challenge when purifying a viral vector. It is necessary to assess both the total recovery of Ad5 capsids and their infective potency across each unit operation. In Table I, this data is presented for each of the ligand densities (Figure 6). Quantitative PCR analysis was used to determine the recovery of total Ad5 VP. At low ligand density fraction LP4 contained the majority of VPs while at medium ligand density it was MP5 and at high ligand density fraction HP6 was found to contain most of the virus particles. TEM analysis was used confirm presence of Ad5 (Figure 7). This increase in fraction number for VP elution with ligand density is anticipated and reflects the chromatograms seen in Figure 6.

Adenovirus 5 particle infectivity was measured by counting β-galactosidase staining in infected cells (Table I). The ratio of viral particles to infective viral particles or units (VP/IVP) is often used as an indicator of product quality. At low ligand density the LP4 fraction contained a ratio of 4.59 VP/IVP, MP5 had 5.12, and HP6 4.00 VP/IVP all are within accepted ranges for clinical use (Kramberger et al., 2015) and despite the different ligand densities presenting unique elution profiles with product eluting at different conductivities, the highest titre peaks (LP4, MP5 and HP6) showed a relatively consistent infective ratio. The highest proportion of packed, non-infective Ad5 capsids were separated in HP7 using high ligand density nanofibers with a coefficient of 16.04 VP/IVP, suggesting clearance of a population of lower quality Ad5. Damaged or immature Ad5, represent important possible product related impurities. Therefore their separation is of particular interest for the manufacture of viral vectors for therapeutic use.

Clearance of host cell proteins (HCPs) a process related impurity of primary importance in the manufacture of a therapeutic biological product is documented in Table 1. Removal across the TFF and chromatography step was high with >95% (compared to non-purified Ad5 feed) of HCPs removed.

The mass balances of packed, infective Ad5 capsid recovery across all nanofibers ligand densities were similarly high (Table I) especially when compared to other membrane adsorbers (P. Nestola et al., 2014) and monoliths (Lucero et al., 2017) with recoveries of 70%, and 34% respectively

Separation of Free Hexon Capsid Protein

Analysis of capsid recovery provides evidence for the separation of free capsid proteins from assembled virus particles. Hexon is a key component within the Ad5 capsid (see Figure 1) but can also be found in non-assembled forms (Klyushnichenko, Bernier, Kamen, & Harmsen, 2001). It has been shown to be immunogenic and represents an important product related impurity (Bradley, Lynch, Iampietro, Borducchi, & Barouch, 2012). A western blot (Figure 8) was used to show the distribution of hexon during the separations shown in Figure 6. Hexon was identified in the purified fractions, LP3, LP4, MP5, and HP6, demonstrated to contain packed and infective Ad5 capsids. Hexon is also found in MP3 and HP4 fractions that do not contain infective Ad5 particles and therefore is free hexon protein that is not incorporated into complete capsids. This suggests with medium and high ligand density nanofibers it was possible to isolate free hexon from capsid bound hexon, it is possible at low ligand density free capsid does not bind and goes straight into the flow through. The ability to resolve free hexon from an adenovirus feed using a DEAE-Fractogel anion exchange was also demonstrated by Green et al. (2002), eluting, as shown here at low ionic strength (<25 mS/cm).

Conclusions

Nanofibers provide a promising scalable capture platform by which to purify Ad5 from HCP and free hexon, producing an enriched product pool with a high product quality as determined by the VP/IVP ratio. Using medium and high ligand density nanofibers it was possible to achieve a separation of product peaks from a hexon rich peak during salt gradient elution. The Ad5 hexon forms the major building block of the virus capsid (>60%)

(Perez-Berna et al., 2012) and non-assembled hexon represents major product impurity due to its antigenic properties. We show that nanofiber materials allow very high infective recoveries of >90%. Critical to this is adsorption time, which when reduced from 24 to 8 min improved recovery from ~50% to >90% and up to 97% for 1 min. The macroporosity, convective mass transfer characteristics and shallow bed height of the nanofibers allows for rapid separations in this manner. Operating under these conditions a 29-fold productivity improvement can be achieved over a classical beaded packed bed resin process. The high recovery achieved across this initial capture step allows for a two or three step chromatography process to readily be considered to meet a given product's specification. The results presented here therefore demonstrate potential clinical utility of this nanofiber adsorbent as a high productivity manufacturing technology for the capture of infective Ad5.

Acknowledgements

This research was supported by the UK Engineering and Physical Sciences Research Council (EPSRC) grant EP/L01520X/1, and Puridify (now part of GE Healthcare), in conjunction with grant EP/N013395/1. We would like to thank Mark Turmaine, for support with electron microscopy.

Conflict of interest

No conflict of interest.

Tables

Table I. The total recoveries of infective Ad5 units (IVP, analysed by β-Gal stain), DNA containing (VP, analysed by qPCR) Ad5 units and the ratio of these two populations within all Ad5 containing peaks separated on low (440 µmol/g), medium (750 µmol/g) and high (1029 µmol/g) Q ligand density nanofibers. No qPCR signal was detected for samples LP3 and MP4. Good amounts of host cell protein was shown to be removed from the Ad5 containing feed, when compared to clarified cell lysate (CCL) Ad5 harvest (1.30E+06 ng/mL) (n=3).

	Ad5 containing sample	Sample Volume (mL)	Infectious particle number (IVP)	Standard Error of the Mean	Total IVP Recovery to IVP recovery from TFF	IVP Recovery Standard Error	Virus Particle Number	Standard Error of the Mean	Total VP Recovery to VP recovery from TFF	VP Recovery Standard Error	Infectivity coefficient (VP/IVP)	Eluted NaCl concentration (M)	HCP conc (ng/mL)	Percentage HCP removal from CCL
	CCL	**Total**	**6.31E+08**	**9.40E+06**	**-**	**-**	**-**	**-**	**-**	**-**	**-**	**N/A**	**1.30E+06**	**0%**
	Feed (TFF)	**Total**	**5.60E+08**	**8.70E+06**	**100.0%**	**1.53%**	**2.39E+09**	**3.30E+07**	**100.0%**	**1.31%**	**4.23**	**N/A**	**3.56E+05**	**72.6%**
Low	LP3	8	1.40E+07	4.00E+06			-	-			-	0.29	3.82E+04	97.1%
Ligand	LP4	8	4.22E+08	8.72E+06			1.94E+09	5.06E+07			4.59	0.49	4.00E+04	96.9%
Density	LP5	6	7.13E+07	8.73E+06			3.26E+08	3.03E+07			4.57	1	4.87E+04	96.3%
		Total	**5.07E+08**		**90.2%**	**3.81%**	**2.27E+09**		**94.8%**	**3.38%**	**4.47**		**4.23E+04**	**96.8%**
Medium	MP4	8	4.20E+07	6.93E+06			-	-			-	0.43	6.28E+04	95.2%
Ligand	MP5	8	4.39E+08	1.51E+07			2.25E+09	2.46E+08			5.12	0.6	3.67E+04	97.2%
Density	MP6	6	3.26E+07	4.99E+06			2.69E+08	3.86E+07			8.25	1	6.05E+04	95.4%
		Total	**5.14E+08**		**91.4%**	**4.81%**	**2.53E+09**		**105.4%**	**11.91%**	**4.93**		**5.33E+04**	**95.9%**
High	HP6	8	4.97E+08	1.48E+07			1.99E+09	4.71E+07			4.00	0.61	3.32E+04	97.5%
Ligand	HP7	6	2.55E+07	5.41E+06			4.09E+08	1.44E+07			16.04	1	5.45E+04	95.8%
Density		**Total**	**5.23E+08**		**92.9%**	**3.59%**	**2.40E+09**		**99.6%**	**2.57%**	**4.59**		**4.39E+04**	**96.6%**

Figures

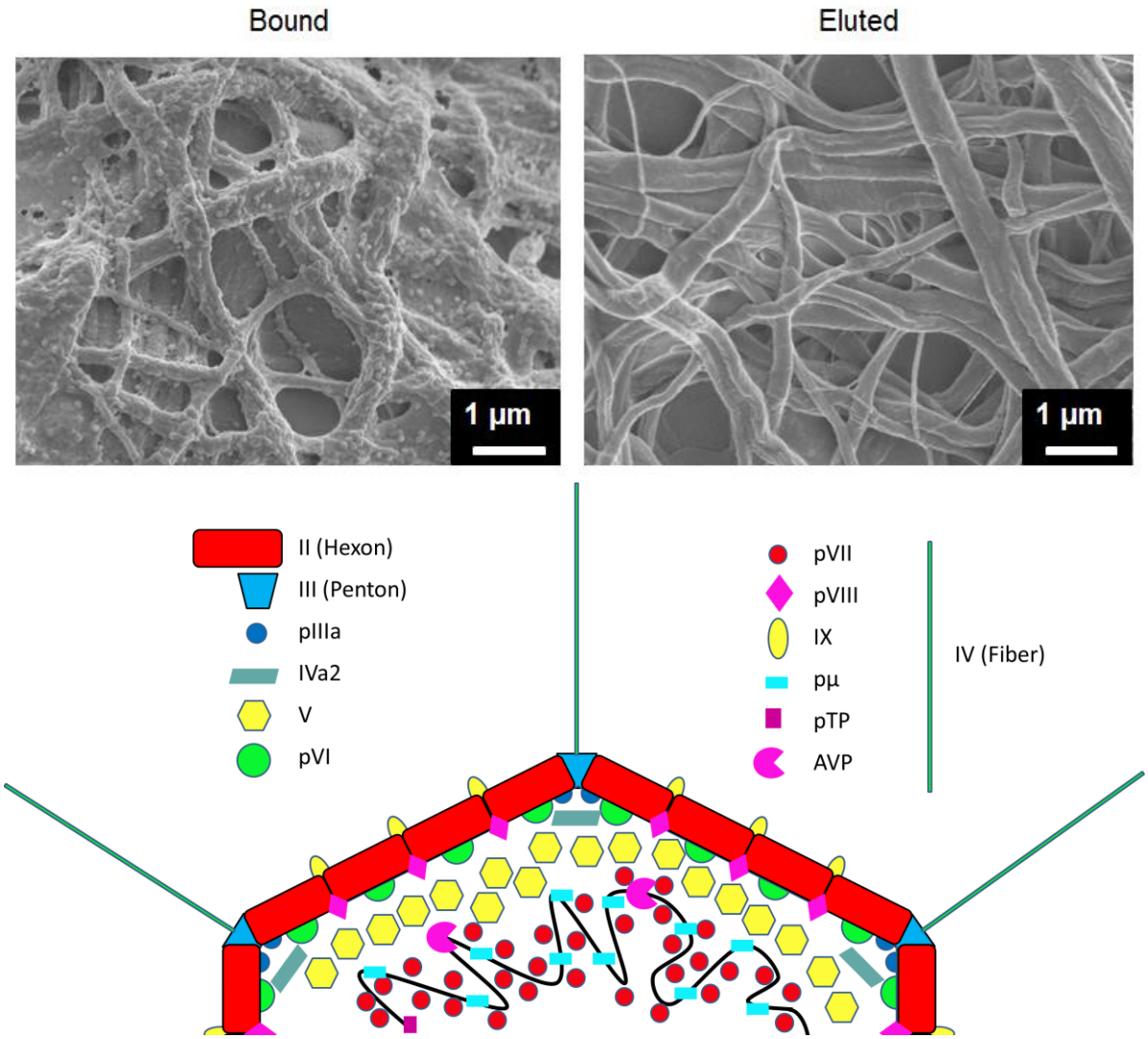

Figure 1. Top - Scanning electron microscopy images of Ad5 bound to Q ligand and eluted from functionalised nanofibers. Bottom – Diagram of adenovirus proteins, highlighting the level of complexity within each virion (diagram combined from Mangel and San Martin (2014); San Martin (2012)). Adenovirus proteins prefixed with a ‘p’ denote proteins that undergo proteolysis by adenovirus maturation protein (AVP) as part of a maturation which

causes a disassociation of the adenovirus genome from the capsid and a capsid stiffening, priming the capsid for uncoating under endosomal acidification.

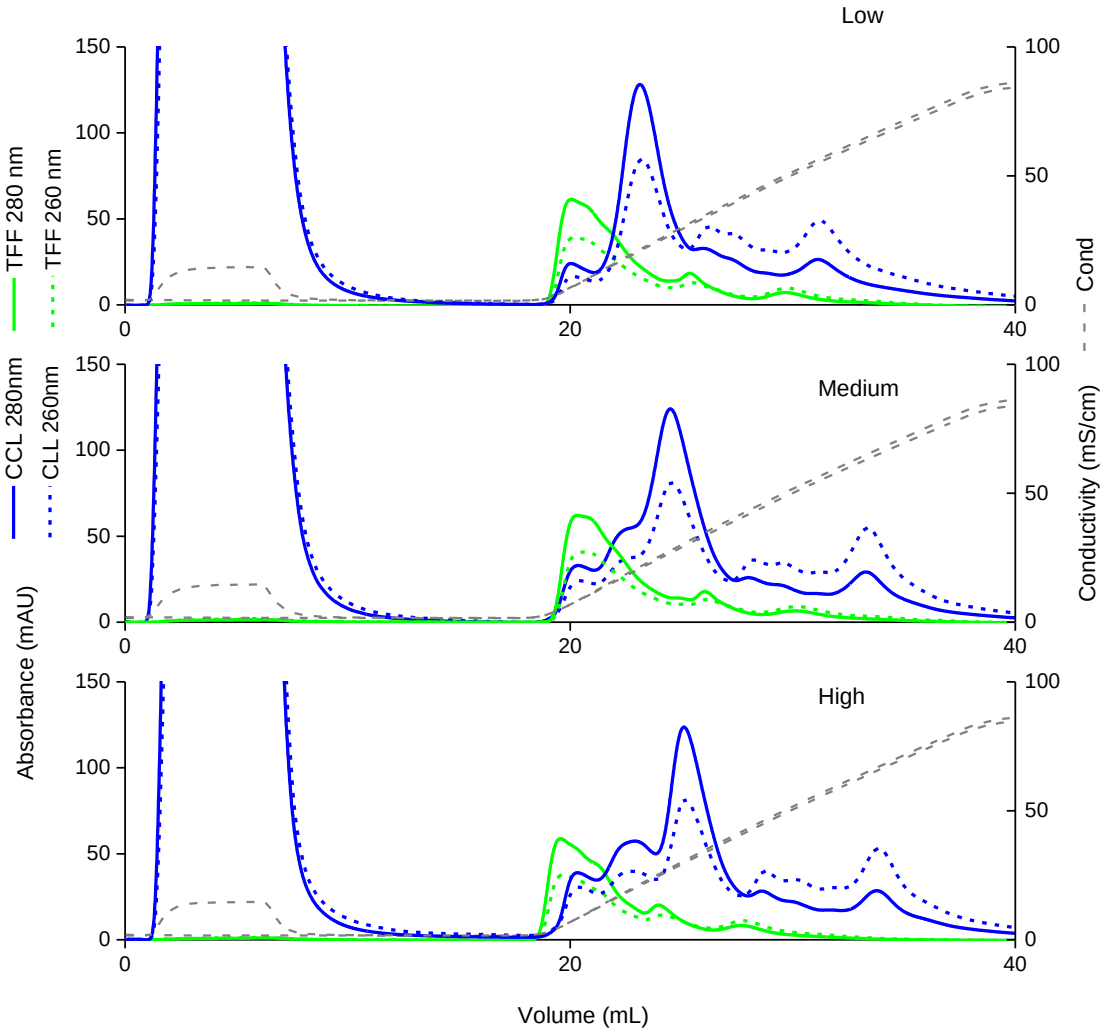

476

477 Figure 2. Elution profile comparison of Ad5 on low (440 µmol/g), medium (750 µmol/g)
478 and high (1029 µmol/g) Q ligand density nanofibers (CV = 0.125 mL). Ad5 was separated
479 from a clarified cell lysate (CCL) and a tangential flow filtration (TFF) UF–DF 500 kDa
480 retentate diafiltered into binding buffer (20 mM Tris, pH 7.4). Loads (5 mL) of both Ad5
481 feeds containing a total load of $5.6 \times 10^8 \pm 5.6 \times 10^7$ IVP were used. Chromatograms were

482 generated using a 20 mL gradient elution at 10 mL/min from 0 M NaCl, 20 mM Tris pH 7.4,

483 to 1 M NaCl, 20 mM Tris pH 7.4 (n=3).

484

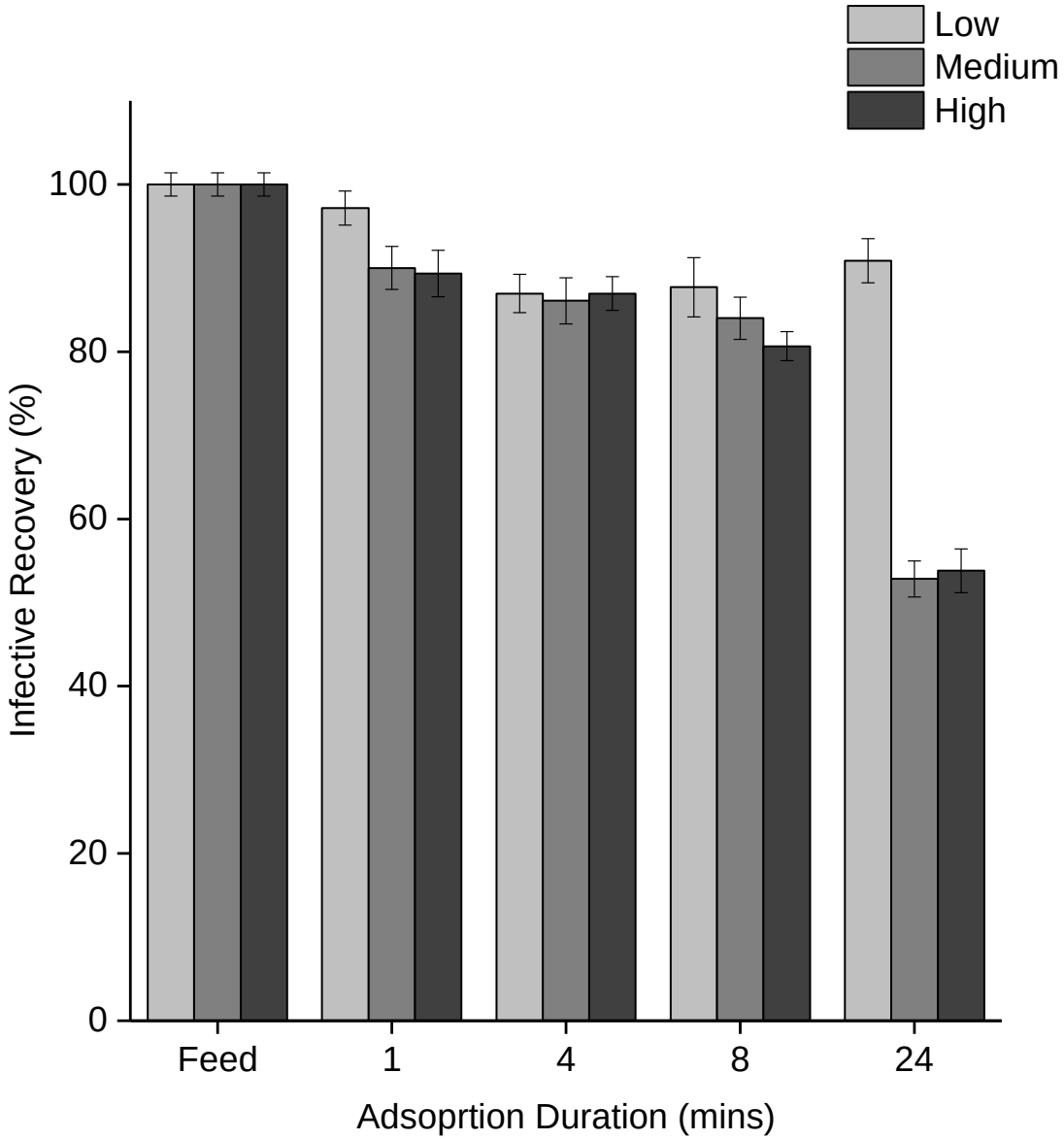

485

486 Figure 3. Recovery of adenovirus 5 infectivity during adsorption to nanofiber based ion
487 exchangers, measured by a cell based β-galactosidase reporter assay. Low (440 µmol/g),
488 medium (750 µmol/g) and high (1029 µmol/g) Q ligand density nanofibers (CV = 0.125
489 mL) were loaded with 6.22 x 10^8 IVP of Ad5 in a clarified feed (n=3).

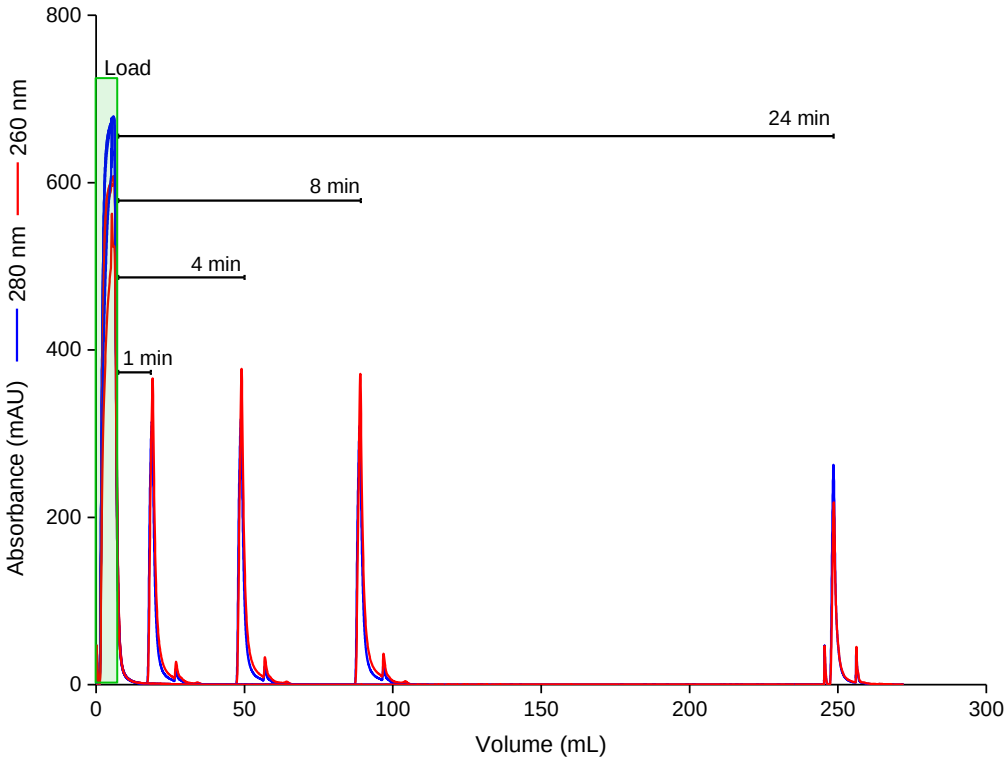

490

491 Figure 4. Elution profile of four chromatography runs of clarified cell lysate Ad5 feed with
492 varying wash durations (10, 40, 80, 240 mL or 1, 4, 8, 24 min) in triplicate for a total of
493 twelve runs for Low (440 µmol/g) charge density.

494

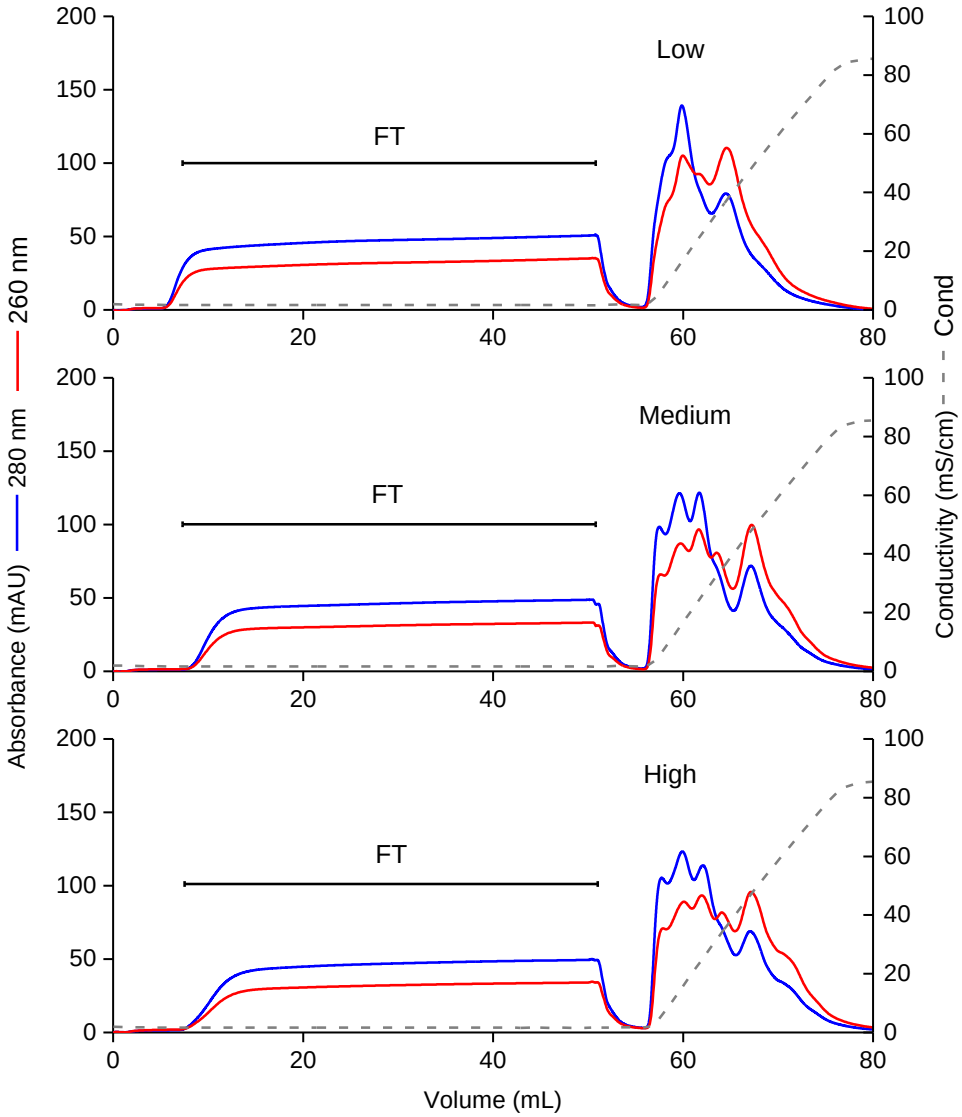

495

496 Figure 5. High loadings of adenovirus feed material to quaternary amine exchange
497 nanofibers. A 50 mL (high volume) TFF Ad5 feed (2.39 x 10^{10} VP, 5.6 x 10^{9} IVP) was

498 separated using low (440 µmol/g), medium (750 µmol/g) and high (1029 µmol/g) Q amine
499 ligand density nanofibers (CV = 0.125 mL). Fiber saturation was not achieved (n=3).

500

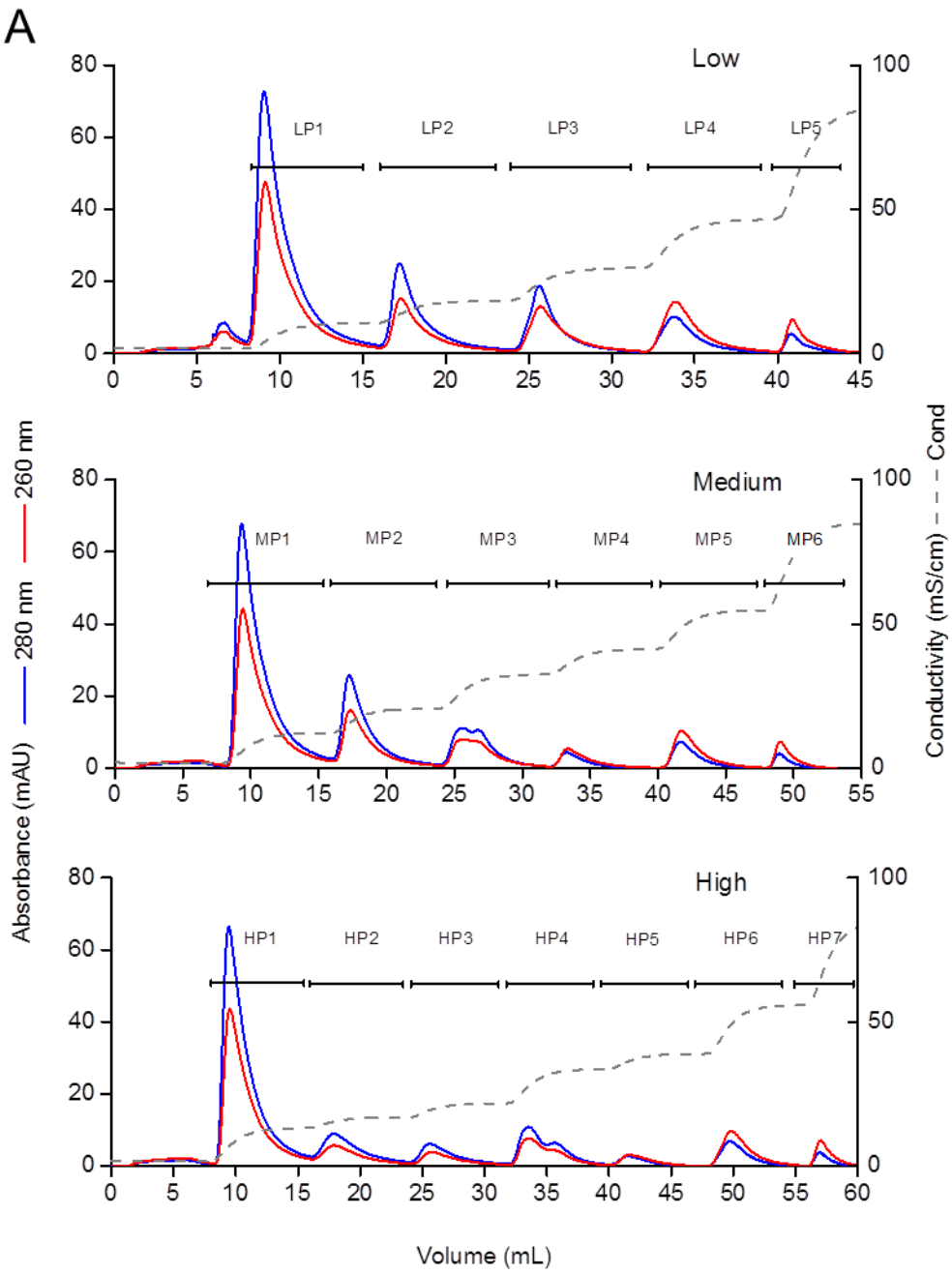

501

502 Figure 6. The impact of increasing Q amine ligand density on the resolution of Ad5 feed
503 components. Elution peak profiles of low (440 µmol/g), medium (750 µmol/g) and high
504 (1029 µmol/g) Q amine ligand density nanofibers were recorded from a chromatography run

505 of 5 mL (2.39 x 10^9 VP, 5.6 x 10^8 IVP) TFF feed loaded onto a 0.125 mL nanofiber column

506 at a flow rate of 10 mL/min (n=3).

507

508 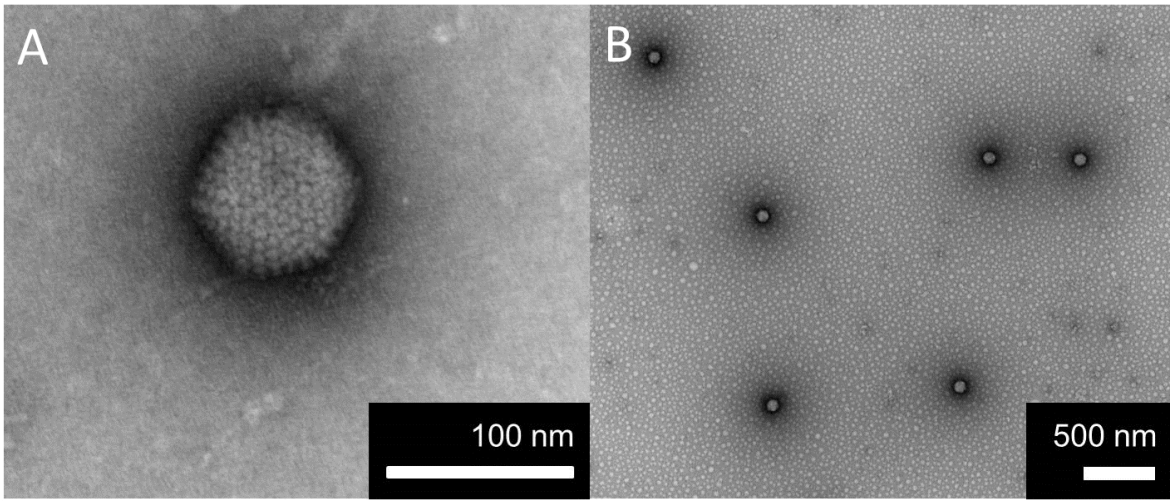

509 Figure 7. High (A) and Low (B) magnification transmission electron microscopy analysis
510 showed the presence of Ad5 particles in fraction HP6.

511
512

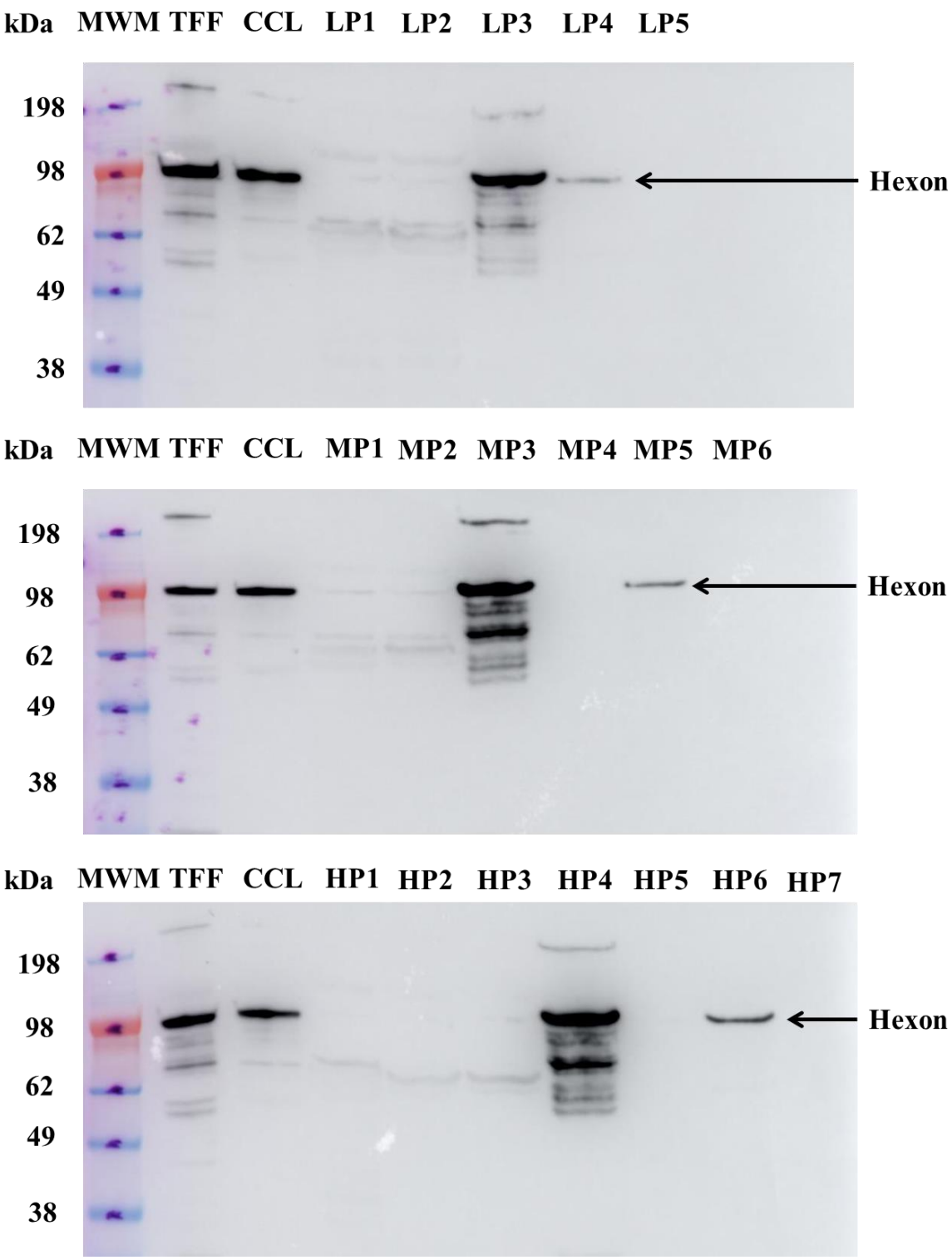
kDa MWM TFF CCL LP1 LP2 LP3 LP4 LP5
198
98
62
49
38
Hexon
kDa MWM TFF CCL MP1 MP2 MP3 MP4 MP5 MP6
198
98
62
49
38
Hexon
kDa MWM TFF CCL HP1 HP2 HP3 HP4 HP5 HP6 HP7
198
98
62
49
38
Hexon

513

514 Figure 8. Western blot using a Hexon antibody with a secondary antibody (rabbit polyclonal
515 antibody) to mouse IgG (HRP-conjugated) showing Adenovirus 5 hexon expression in
516 purified fractions from low (440 µmol/g), medium (750 µmol/g) and high (1029 µmol/g) Q
517 ligand density nanofibers collected from step elution chromatograms (n=3). A molecular
518 weight marker (MWM) and Ad5 from a clarified cell lysate (CCL) and a tangential flow
519 filtration (TFF) UF–DF 500 kDa retentate diafiltered into binding buffer (20 mM Tris, pH
520 7.4) was also loaded.

521

References

Bo, H., Chen, J., Liang, T., Li, S., Shao, H., & Huang, S. (2015). Chromatographic purification of adenoviral vectors on anion-exchange resins. *Eur J Pharm Sci, 67*, 119-125. doi: 10.1016/j.ejps.2014.11.004

Bradley, R. R., Lynch, D. M., Iampietro, M. J., Borducchi, E. N., & Barouch, D. H. (2012). Adenovirus serotype 5 neutralizing antibodies target both hexon and fiber following vaccination and natural infection. *Journal of Virology, 86*(1), 625-629.

Chen, H., Marino, S., & Ho, C. Y. (2016). 97. Large Scale Purification of AAV with Continuous Flow Ultracentrifugation. *Molecular Therapy, 24*, S42.

Crystal, R. G. (2014). Adenovirus: the first effective in vivo gene delivery vector. *Hum Gene Ther, 25*(1), 3-11. doi: 10.1089/hum.2013.2527

Green, A. P., Huang, J. J., Scott, M. O., Kierstead, T. D., Beaupre, I., Gao, G. P., & Wilson, J. M. (2002). A new scalable method for the purification of recombinant adenovirus vectors. *Hum Gene Ther, 13*(16), 1921-1934. doi: 10.1089/10430340260355338

Habib, N. A., Sarraf, C. E., Mitry, R. R., Havlik, R., Nicholls, J., Kelly, M., . . . Salama, H. (2001). E1B-deleted adenovirus (dl 1520) gene therapy for patients with primary and secondary liver tumors. *Human Gene Therapy, 12*(3), 219-226.

Hardick, O., Dods, S., Stevens, B., & Bracewell, D. G. (2013). Nanofiber adsorbents for high productivity downstream processing. *Biotechnology and bioengineering, 110*(4), 1119-1128. doi: 10.1002/bit.24765

Hardick, O., Dods, S., Stevens, B., & Bracewell, D. G. (2015). Nanofiber adsorbents for high productivity continuous downstream processing. *Journal of Biotechnology, 213*, 74-82. doi: https://doi.org/10.1016/j.jbiotec.2015.01.031

Hardick, O., Stevens, B., & Bracewell, D. (2011). Nanofibre fabrication in a temperature and humidity controlled environment for improved fibre consistency. *Journal of Materials Science, 46*(11), 3890-3898. doi: 10.1007/s10853-011-5310-5

Huang, Y., Bi, J., Zhou, W., Li, Y., Wang, Y., Ma, G., & Su, Z. (2006). Improving recovery of recombinant hepatitis B virus surface antigen by ion-exchange chromatographic supports with low ligand density. *Process Biochemistry, 41*(11), 2320-2326. doi: https://doi.org/10.1016/j.procbio.2006.06.004

Keeler, A. M., ElMallah, M. K., & Flotte, T. R. (2017). Gene therapy 2017: Progress and future directions. *Clinical and Translational Science*.

Klyushnichenko, V., Bernier, A., Kamen, A., & Harmsen, E. (2001). Improved high-performance liquid chromatographic method in the analysis of adenovirus particles. *J Chromatogr B Biomed Sci Appl, 755*(1-2), 27-36.

Kramberger, P., Urbas, L., & Štrancar, A. (2015). Downstream processing and chromatography based analytical methods for production of vaccines, gene therapy vectors, and bacteriophages. *Human vaccines & immunotherapeutics, 11*(4), 1010-1021.

Lee, C. S., Bishop, E. S., Zhang, R., Yu, X., Farina, E. M., Yan, S., . . . He, T.-C. (2017). Adenovirus-mediated gene delivery: Potential applications for gene and cell-based therapies in the new era of personalized medicine. *Genes & Diseases, 4*(2), 43-63. doi: https://doi.org/10.1016/j.gendis.2017.04.001

Lucero, A. T., Mercado, S. A., Sánchez, A. C., Contador, C. A., Andrews, B. A., & Asenjo, J. A. (2017). Purification of adenoviral vector serotype 5 for gene therapy against

alcoholism using anion exchange chromatography. *Journal of Chemical Technology & Biotechnology, 92*(9), 2445-2452. doi: doi:10.1002/jctb.5255

Lusky, M. (2005). Good manufacturing practice production of adenoviral vectors for clinical trials. *Hum Gene Ther, 16*(3), 281-291. doi: 10.1089/hum.2005.16.281

Mangel, W. F., & San Martin, C. (2014). Structure, function and dynamics in adenovirus maturation. *Viruses, 6*(11), 4536-4570. doi: 10.3390/v6114536

Matsumoto, H., Wakamatsu, Y., Minagawa, M., & Tanioka, A. (2006). Preparation of ion-exchange fiber fabrics by electrospray deposition. *J Colloid Interface Sci, 293*(1), 143-150. doi: 10.1016/j.jcis.2005.06.022

McNally, D., Darling, D., Farzaneh, F., Levison, P., & Slater, N. (2014). Optimised concentration and purification of retroviruses using membrane chromatography. *Journal of Chromatography A, 1340*, 24-32.

Nestola, P., Silva, R. J., Peixoto, C., Alves, P. M., Carrondo, M. J., & Mota, J. P. (2014). Adenovirus purification by two-column, size-exclusion, simulated countercurrent chromatography. *Journal of Chromatography A, 1347*, 111-121.

Nestola, P., Villain, L., Peixoto, C., Martins, D. L., Alves, P. M., Carrondo, M. J., & Mota, J. P. (2014). Impact of grafting on the design of new membrane adsorbers for adenovirus purification. *J Biotechnol, 181*, 1-11. doi: 10.1016/j.jbiotec.2014.04.003

Peixoto, C., Ferreira, T. B., Sousa, M. F. Q., Carrondo, M. J. T., & Alves, P. M. (2008). Towards purification of adenoviral vectors based on membrane technology. *Biotechnology Progress, 24*(6), 1290-1296. doi: 10.1002/btpr.25

Perez-Berna, A. J., Ortega-Esteban, A., Menendez-Conejero, R., Winkler, D. C., Menendez, M., Steven, A. C., . . . San Martin, C. (2012). The role of capsid maturation on adenovirus priming for sequential uncoating. *J Biol Chem, 287*(37), 31582-31595. doi: 10.1074/jbc.M112.389957

Rathore, A., & Sofer, G. (2005). Life span studies for chromatography and filtration media. *Process Validation in Manufacturing of Biopharmaceuticals*, 169-204.

Ruckenstein, E., & Guo, W. (2004). Cellulose and glass fiber affinity membranes for the chromatographic separation of biomolecules. *Biotechnol Prog, 20*(1), 13-25. doi: 10.1021/bp030055f

Ryu, Y. J., Kim, H. Y., Lee, K. H., Park, H. C., & Lee, D. R. (2003). Transport properties of electrospun nylon 6 nonwoven mats. *European Polymer Journal, 39*(9), 1883-1889. doi: https://doi.org/10.1016/S0014-3057(03)00096-X

San Martin, C. (2012). Latest insights on adenovirus structure and assembly. *Viruses, 4*(5). doi: 10.3390/v4050847

Smaill, F., Jeyanathan, M., Smieja, M., Medina, M. F., Thanthrige-Don, N., Zganiacz, A., . . . Puri, L. (2013). A human type 5 adenovirus–based tuberculosis vaccine induces robust T cell responses in humans despite preexisting anti-adenovirus immunity. *Science translational medicine, 5*(205), 205ra134-205ra134.

Stanelle, R., M Straut, C., & Marcus, R. (2007). *Nylon-6 Capillary-Channeled Polymer Fibers as a Stationary Phase for the Mixed-Mode Ion Exchange/Reversed-Phase Chromatography Separation of Proteins* (Vol. 45).

Trilisky, E. I., & Lenhoff, A. M. (2009). Flow-dependent entrapment of large bioparticles in porous process media. *Biotechnology and bioengineering, 104*(1), 127-133. doi: 10.1002/bit.22370

612 Vellinga, J., Smith, J. P., Lipiec, A., Majhen, D., Lemckert, A., van Ooij, M., . . . Havenga,
613 M. (2014). Challenges in manufacturing adenoviral vectors for global vaccine
614 product deployment. *Hum Gene Ther, 25*(4), 318-327. doi: 10.1089/hum.2014.007
615 Vicente, T., Fáber, R., Alves, P. M., Carrondo, M. J. T., & Mota, J. P. B. (2011). Impact of
616 ligand density on the optimization of ion-exchange membrane chromatography for
617 viral vector purification. *Biotechnology and bioengineering, 108*(6), 1347-1359. doi:
618 doi:10.1002/bit.23058
619 Vicente, T., Roldão, A., Peixoto, C., Carrondo, M. J. T., & Alves, P. M. (2011). Large-scale
620 production and purification of VLP-based vaccines. *Journal of Invertebrate*
621 *Pathology, 107, Supplement*(0), S42-S48. doi:
622 http://dx.doi.org/10.1016/j.jip.2011.05.004
623 Vincent, D., Kramberger, P., Hudej, R., Štrancar, A., Wang, Y., Zhou, Y., & Velayudhan,
624 A. (2017). The development of a monolith-based purification process for
625 Orthopoxvirus vaccinia virus Lister strain. *Journal of Chromatography A*. doi:
626 https://doi.org/10.1016/j.chroma.2017.09.003
627 Wang, J., Faber, R., & Ulbricht, M. (2009). Influence of pore structure and architecture of
628 photo-grafted functional layers on separation performance of cellulose-based
629 macroporous membrane adsorbers. *J Chromatogr A, 1216*(37), 6490-6501. doi:
630 10.1016/j.chroma.2009.07.042
631 Wen-Chien, L., Chang-Hung, L., Ruoh-Chyu, R., & Keh-Ying, H. (1995). High-
632 performance affinity chromatography of proteins on non-porous polystyrene beads.
633 *Journal of Chromatography A, 704*(2), 307-314. doi: https://doi.org/10.1016/0021-
634 9673(95)00267-Q
635 Whitfield, R. J., Battom, S. E., Barut, M., Gilham, D. E., & Ball, P. D. (2009). Rapid high-
636 performance liquid chromatographic analysis of adenovirus type 5 particles with a
637 prototype anion-exchange analytical monolith column. *Journal of Chromatography*
638 *A, 1216*(13), 2725-2729. doi: 10.1016/j.chroma.2008.11.010
639 Wickramasinghe, S. R., Carlson, J. O., Teske, C., Hubbuch, J., & Ulbricht, M. (2006).
640 Characterizing solute binding to macroporous ion exchange membrane adsorbers
641 using confocal laser scanning microscopy. *Journal of Membrane Science, 281*(1-2),
642 609-618. doi: 10.1016/j.memsci.2006.04.032

643

644